ELSEVIER

Chemical Engineering Journal 87 (2002) 49–59

Chemical Engineering Journal

www.elsevier.com/locate/cej

Modeling of catalytic reactor for oxidative coupling of methane using La_2O_3/CaO catalyst

Ching Thian Tye, Abdul Rahman Mohamed, Subhash Bhatia*

School of Chemical Engineering, Universiti Sains Malaysia, Engineering Campus, 14300 Nibong Tebal, Seberang Prai Selatan, Pulau Pinang, Malaysia

Received 20 March 2001; accepted 20 June 2001

Abstract

A one-dimensional model for the oxidative coupling of methane (OCM) over La_2O_3/CaO catalyst in fixed bed reactor has been developed. This model was tested for isothermal, adiabatic and non-isothermal operation modes. The parameters studied were methane to oxygen (CH_4/O_2) ratio, temperature, space velocity, dilution effect of N_2 and H_2O in the feed. High CH_4/O_2 ratio favored the OCM reaction but gave low yield of ethylene due to insufficient oxygen under isothermal mode. Conversion, selectivity and yield increased with the temperature and a maximum value of yield was obtained at 1098 K. The presence of inert N_2 gas and H_2O in feed gave positive effect to the yield in the process. Non-isothermal and adiabatic operations gave a temperature rise during OCM reaction which led to series of reactions that affected the system conversion, yield and selectivity of the desired product. Therefore, feed temperature, CH_4/O_2 feed ratio and contact time are important parameters in order to control reactor run-away conditions. © 2002 Elsevier Science B.V. All rights reserved.

Keywords: Modeling; Fixed bed catalytic reactor; Oxidative coupling of methane; Ethylene

1. Introduction

Synthesis of ethane and ethylene by oxidative coupling of methane (OCM) offers a potential economical route for conversion of chemicals from natural gas. Due to the complex oxidation and heterogeneous catalytic reaction, the process suffers from low selectivity and yield of ethylene and ethane. A large number of catalysts and their kinetics of this reaction have been reported [1–4]. However, there is still research going on to improve the selectivity and yield of C_2 products towards an economical industrialization.

Reactor configuration and mode of operation were found to play a crucial role in producing high yield and selectivity of ethylene production in OCM reaction. Various types of reactors have been considered and simulated [5–8]. The reactors used were fixed bed, fluidized bed, membrane reactor, reverse flow reactor and counter-current moving-bed reactor. However, fixed bed reactor has been widely used for experimental studies of OCM reaction due to its easy operation. OCM has been considered a heterogeneous reaction and non-catalyzed gas-phase reactions are considered for OCM process modeling.

In the present research, comprehensive study on the performance of the catalytic fixed-bed reactor has been undertaken by modeling and simulating the OCM reaction under different conditions. A plug flow fixed bed catalytic reactor model has been proposed. The model developed has been tested for isothermal and non-isothermal operation modes of the reactor. The model is useful for prediction of reactor performance for OCM reaction under different modes of operation.

2. Kinetics and reactor mathematical model

There is considerable information in the literature that deals with reaction kinetics of oxidative coupling of methane. The kinetic data used in the present study were reported by Stansch et al. [9] using La_2O_3/CaO catalyst and the model used was one-dimensional plug flow model.

3. Oxidative coupling of methane (OCM) kinetic model on La_2O_3/CaO catalyst

The kinetics of OCM on La_2O_3/CaO catalyst involves many species. A set of 10-step kinetic model of OCM over La_2O_3/CaO catalyst was reported by Stansch et al. [9]. It

---

* Corresponding author. Tel.: +60-4-5937788; fax: +60-4-594.
E-mail address: sbhatia@pl.jaring.my (S. Bhatia).

PII: S1385-8947(01)00191-7

Nomenclature

c_p	specific heat, (kJ mol^{-1} K).
c_j^0	initial concentration ratio of j
C_j	concentration of species j (mol m^{-3})
d_p	pellet diameter (m)
d_t	tube diameter (m)
ΔH_{Rij}	heat of reaction (kJ mol^{-1})
m_cat	catalyst weight (g)
P_j	partial pressure of j (Pa)
$r_{\mathrm{c},i}$	rate of formation of catalytic reaction j (mol g^{-1} s)
$r_{\mathrm{g},i}$	rate of formation of gas-phase reaction j (mol g^{-1} s)
Re	Reynold number
R_{ij}	rate of formation of component j in reaction i step (mol g^{-1} s)
S_{C_2}	selectivity of ethylene and ethane
S_j	selectivity of j species
T	temperature (K)
T_ex	external temperature (K)
T^0	feed temperature (K)
u_s	superficial velocity (m s^{-1})
U	overall heat transfer coefficient (W m^{-2} K)
X_j	conversion of j
Y_{C_2}	yield of ethylene and ethane
Y_j	yield of j
z	distance from the start of catalyst bed (m)

Greek letters

α_j	stoichiometric coefficient of component j
ε_b	catalyst bed porosity
ρ_b	density of catalyst in the bed (g m^{-3})
ρ_g	density of system gas (kg m^{-3})
υ_STP	volummetric flow rate under standard temperature condition (m^3 s^{-1})
ψ	shape factor

describes the differential rates of formation for different species in the La_2O_3/CaO packed bed reactor under wide range of experimental conditions ($1 < p_{O_2} < 20\,\mathrm{kPa}$, $10 < p_{CH_4} < 95\,\mathrm{kPa}$, $973 < T < 1228\,\mathrm{K}$ and $0.76 \leq m_\mathrm{cat}/\upsilon_\mathrm{STP} \leq 250\,\mathrm{kg\,s\,m^{-3}}$). The kinetic model included thermal cracking, steam reforming and water gas shift reactions. There were catalytic reaction rates for all the reactions except reaction Step 7, which is a gas-phase reaction. It is the thermal dehydrogenation of ethane occurring under high temperature. The kinetic model considered the following set of stochiometric equations:

$$\text{Step 1}: \quad CH_4 + 2O_2 \rightarrow CO_2 + 2H_2O \tag{1}$$

$$\text{Step 2}: \quad 2CH_4 + 0.5O_2 \rightarrow C_2H_6 + H_2O \tag{2}$$

$$\text{Step 3}: \quad CH_4 + O_2 \rightarrow CO + H_2O + H_2 \tag{3}$$

$$\text{Step 4}: \quad CO + 0.5O_2 \rightarrow CO_2 \tag{4}$$

$$\text{Step 5}: \quad C_2H_6 + 0.5O_2 \rightarrow C_2H_4 + H_2O \tag{5}$$

$$\text{Step 6}: \quad C_2H_4 + 2O_2 \rightarrow 2CO + 2H_2O \tag{6}$$

$$\text{Step 7}: \quad C_2H_6 \rightarrow C_2H_4 + H_2 \tag{7}$$

$$\text{Step 8}: \quad C_2H_4 + 2H_2O \rightarrow 2CO + 4H_2 \tag{8}$$

$$\text{Step 9}: \quad CO + H_2O \rightarrow CO_2 + H_2 \tag{9}$$

$$\text{Step 10}: \quad CO_2 + H_2 \rightarrow CO + H_2O \tag{10}$$

The reaction rates for each step are given below:

$$r_j = \frac{k_{0,j}\,e^{-E_{a,j}/RT} p_\mathrm{C}^{m_j} p_{O_2}^{n_j}}{(1 + K_{j,CO_2}\,e^{-\Delta H_{\mathrm{ad},CO_2,j}/RT} p_{CO_2})^2}, \quad j = 1, 3-6 \tag{11}$$

$$r_2 = \frac{k_{0,2}\,e^{-E_{a,2}/RT}(K_{0,O_2}\,e^{-\Delta H_{\mathrm{ad},O_2}/RT} p_{O_2})^{n_2} p_{CH_4}}{[1 + (K_{0,O_2}\,e^{-\Delta H_{\mathrm{ad},O_2}/RT} p_{O_2})^n + K_{j,CO_2}\,e^{-\Delta H_{\mathrm{ad},O_2,j}/\mathrm{RT}} p_{O_2}]^2} \tag{12}$$

$$r_7 = k_{0,7}\,e^{-E_{a,7}/RT} p_{C_2H_6} \tag{13}$$

$$r_8 = k_{0,8}\,e^{-E_{a,8}/RT} p_{C_2H_6}^{m_8} p_{H_2O}^{n_8} \tag{14}$$

$$r_9 = k_{0,9}\,e^{-E_{a,9}/RT} p_{CO}^{m_9} p_{H_2O}^{n_9} \tag{15}$$

$$r_{10} = k_{0,10}\,e^{-E_{a,10}/RT} p_{CO_2}^{m_{10}} p_{H_2}^{n_{10}} \tag{16}$$

The kinetic parameters used for the above reaction scheme are presented in Table 1.

4. Reactor model equations

A one-dimensional model was developed to simulate the heterogeneous reactions without diffusional resistance. The system was assumed to be under steady state. Simulation was carried out for a plug flow reactor packed with La_2O_3/CaO catalyst. The kinetic model involved both catalytic and gas-phase reactions. Formulation of the model equations is given below.

Mass balance:

$$-u_\mathrm{s}\frac{\mathrm{d}C_j}{\mathrm{d}z} - \rho_\mathrm{b} r_{\mathrm{c},j} + \varepsilon_\mathrm{b} r_{\mathrm{g},j} = 0 \tag{17}$$

Energy balance:

- for adiabatic:

$$-u_\mathrm{s}\rho_\mathrm{g}\sum c_\mathrm{p}\frac{\mathrm{d}T}{\mathrm{d}z} + \rho_\mathrm{b}\sum r_{\mathrm{c},j}(-\Delta H) + \varepsilon_\mathrm{b}\sum r_{\mathrm{g},j}(-\Delta H) = 0 \tag{18}$$

- for non-adiabatic/non-isothermal:

$$-u_\mathrm{s}\rho_\mathrm{g}\sum c_\mathrm{p}\frac{\mathrm{d}T}{\mathrm{d}z} + \rho_\mathrm{b}\sum r_{\mathrm{c},j}(-\Delta H) + \varepsilon_\mathrm{b}\sum r_{\mathrm{g},j}(-\Delta H) - 4\frac{U}{d_\mathrm{t}}(T - T_\mathrm{ex}) = 0 \tag{19}$$

Table 1
Kinetic parameters [9]

Step	$K_{0,j}$ (mol g^{-1} s^{-1} Pa$^{-(m+n)}$)	$E_{a,j}$ (kJ mol^{-1})	m_j	n_j	K_{j,CO_2} (Pa^{-1})	$\Delta H_{ad,CO_2}$ (kJ mol^{-1})	K_{j,O_2} (Pa^{-1})	$\Delta H_{ad,O_2}$ (kJ mol^{-1})
1	0.20×10^{-5}	48	0.24	0.76	0.25×10^{-12}	−175		
2	23.2	182	1.0	0.40	0.83×10^{-13}	−186	0.23×10^{-11}	−124
3	0.52×10^{-6}	68	0.57	0.85	0.36×10^{-13}	−187		
4	0.11×10^{-3}	104	1.0	0.55	0.40×10^{-12}	−168		
5	0.17	157	0.95	0.37	0.45×10^{-12}	−166		
6	0.06	166	1.0	0.96	0.16×10^{-12}	−211		
7	1.2×10^{7}[a]	226						
8	9.3×10^{3}	300	0.97	0				
9	0.19×10^{-3}	173	1.0	1.0				
10	0.26×10^{-1}	220	1.0	1.0				

[a] Units are mol s^{-1} m^{-3} Pa^{-1}.

Momentum balance (Ergun's equation):

$$-\frac{dP}{dz} = \frac{\rho_g u_s^2}{\psi d_p}\left(\frac{1-\varepsilon}{\varepsilon^3}\right)\left[\frac{150(1-\varepsilon)}{\psi Re} + 1.75\right] \qquad (20)$$

The net rates of formation of each component, j was given by $r_j = \sum a_j R_{ij}$ where i represent reaction in each step. The specific heat and heat of reactions are computed as a function of temperature. The reaction rates were expressed as a function of partial pressure and temperature. To convert the partial pressure of each species to concentration, the relationship of ideal gas law, $p_j = C_j RT$ was used.

The model was used to simulate OCM reaction under three operational modes. These were isothermal, adiabatic and non-isothermal/non-adiabatic operation. Simulation of isothermal operation was considered to be appropriate to study the influence of the changes in different operating variables without added temperature effect. Since most of the OCM laboratory experiments were carried and reported under assumption of the isothermal condition. For isothermal simulation, only mass balance and momentum equations (Eqs. (17) and (20)) were considered.

The overall oxidative coupling process is highly exothermic and isothermal operation would be difficult to be achieved. Adiabatic operation is easier to bring into practice because of the simplicity of construction of the reactor. In the reactor model for adiabatic operation, an energy balance equation (Eq. (18)) is considered besides mass and momentum balance equations.

Since OCM reaction is highly exothermic, therefore, hot spot could be developed in the reactor. In order to limit the hot spots, which could result to run away condition, part of heat released during the coupling reaction needed to be removed from the reactor. This brought to the simulation of non-isothermal and non-adiabatic operation. The reactor model for OCM process for non-isothermal operation is basically same as the adiabatic model. For non-isothermal model, energy balance Eq. (19) was used instead of Eq. (18).

The initial conditions, at the entrance of the reactor, $z = 0$, are as follows:

$$C_n = C_n^0, \qquad C_m = C_m^0, \qquad T = T^0, \quad \text{and} \quad P = P^0$$

where n represents reactants as well as inert in feed and m represents products. Temperature needed as an initial condition only in non-isothermal operation.

Inert gas like nitrogen is normally fed into the reactor along with methane and oxygen in the oxidative coupling process. It carries the task of controlling the temperature in the reactor, since OCM is a highly exothermic reaction. The presence of certain amount of inert gas has some positive effect to the oxidative process as well.

The performance of the reactor is evaluated by the conversion of reactants as well as selectivity and yield of products. The conversion is defined as the fraction of the reactant reacted to the reactant fed. For example the conversion of methane is

$$X_{CH_4} = \frac{C_{CH_4}^0 - C_{CH_4}}{C_{CH_4}^0} \qquad (21)$$

and the C_2 selectivity is defined as C_2 product formed per reactant consumed.

$$S_{C_2} = \frac{2C_{C_2H_4} + 2C_{C_2H_6}}{C_{CH_4}^0 - C_{CH_4}} \qquad (22)$$

while yield referred to the specific product formed per reactant fed.

$$Y_{C_2H_4} = \frac{2C_{C_2H_4}}{C_{CH_4}^0} \qquad (23)$$

The differential Eqs. (17) to (20) were solved using adaptive Runge–Kutta method using MathCAD 8.0.

5. Results and discussion

Simulations were carried out for OCM in fixed bed rector for isothermal, adiabatic and non-adiabatic operations. The reactor chosen for the study was a conventional tubular reactor packed with La_2O_3/CaO catalyst. The reactor was operated at 110 kPa total pressure.

Table 2
Reactor parameters and constants

Properties	Dimension
Inner diameter (mm)	6
Pressure (kPa)	110
Length of catalyst bed (mm)	2–54
Catalyst weight, m_{cat} (g)	0.007–1.000
Flow rate (STP), υ_{STP} ($m^3\,s^{-1}$)	4×10^{-6}–13×10^{-4}
Catalyst size (mm)	0.25–0.35
Catalyst density ($kg\,m^{-3}$)	3600

6. Validation of kinetic and reactor model

The validity of the model was tested by comparing the theoretical predictions of differential kinetics with experimental results for OCM in the fixed bed reactor packed with La_2O_3/CaO catalyst reported by Stansch [10]. In order to compare simulated data with the experimental data, the actual reactor dimensions and conditions were used in the simulation, as presented in Table 2.

The model was found to fit the experimental data plausibly. Table 3 shows a set of simulated and experimental data compared under same space velocity. In the experiment, methane and oxygen were fed with nitrogen gas as an inert into the reactor. All these runs were operated at a feed flow rate of $4\,cm^3\,s^{-1}$ over 14.8 mg of La_2O_3/CaO catalyst. It was found that for the case of high methane to oxygen ratio, the present model fits the experimental data well for run number 1, 2 and 3 compared to run 4, 5 and 6. The prediction was generally lower for low methane to oxygen ratio. When the temperature increased, the error between simulated and experimental results was within 20%. The OCM kinetic equation proposed by Stansch et al. [9] predicts the experimental results reasonably.

The error differences between the simulated and experimental data can be caused due to several reasons. Pre-and post-catalytic zone reactions were not considered into account in the model and simulation. The gas-phase reaction considered in the model was the interstitial gas-phase reaction within the catalytic bed. There could be reactions in gas-phase that occurred before reactants entering into the catalytic bed, such as gas-phase oxidation of methane. This deviate the initial conditions as assumed in the simulation. The same holds in the post-catalytic zone of reactor. The gas-phase reactions like thermal decomposition and combustion contributed some difference to the catalytic bed performance. These were not considered in the simulation. This resulted in the difference between the simulated and experimental data. Besides, OCM reaction is a gas/solid heterogeneous reaction. Mass and heat transfer resistances as well as the axial and radial dispersion could affect the performance and contributed to the error differences.

7. Isothermal fixed bed reactor simulation results

7.1. Effect of methane to oxygen ratio in feed

A number of simulations were carried out with varying feed composition CH_4/O_2 ratio. The results are plotted in Fig. 1. It shows that, when the feed of CH_4/O_2 ratio is increased, (i) the conversion of methane drops substantially, (ii) the selectivity for the C_2 product increases markedly and (iii) the yield for C_2 product decreases. These results show that higher conversion of methane and C_2 product yield is obtained at higher oxygen ratio (low CH_4/O_2 ratio). This observation agreed with experimental observations reported [1,3]. The highest methane conversion observed was at 45% with 19% of C_2 yield at CH_4/O_2 ratio of 2. Graphs are

Table 3
Comparison between experimental and simulated data

	Runs					
	1 (1023 K)	2 (1073 K)	3 (1103 K)	4 (973 K)	5 (1023 K)	6 (1103 K)
Feed mole ratio[a]						
CH_4	0.612	0.612	0.612	0.699	0.699	0.699
O_2	0.051	0.051	0.051	0.095	0.095	0.095
N_2	0.337	0.337	0.337	0.206	0.206	0.206
CH_4 conversion (%)						
Experimental[b]	4.9	7.9	9.9	4.1	7.1	14.4
Simulated	4.9	8.5	10.9	3.0	5.8	13.7
C_2 selectivity (%)						
Experimental[b]	55.6	69.2	72.5	35.6	53.7	69.6
Simulated	54.6	64.5	66.4	31.7	46.4	58.9
C_2 yield (%)						
Experimental[b]	2.7	5.5	7.2	1.5	3.8	10
Simulated	2.7	5.5	7.3	1.0	2.7	8.1

[a] At $m_{cat}/\upsilon_{STP} = 3.70\,kg\,s\,m^{-3}$.
[b] Experimental data [10].

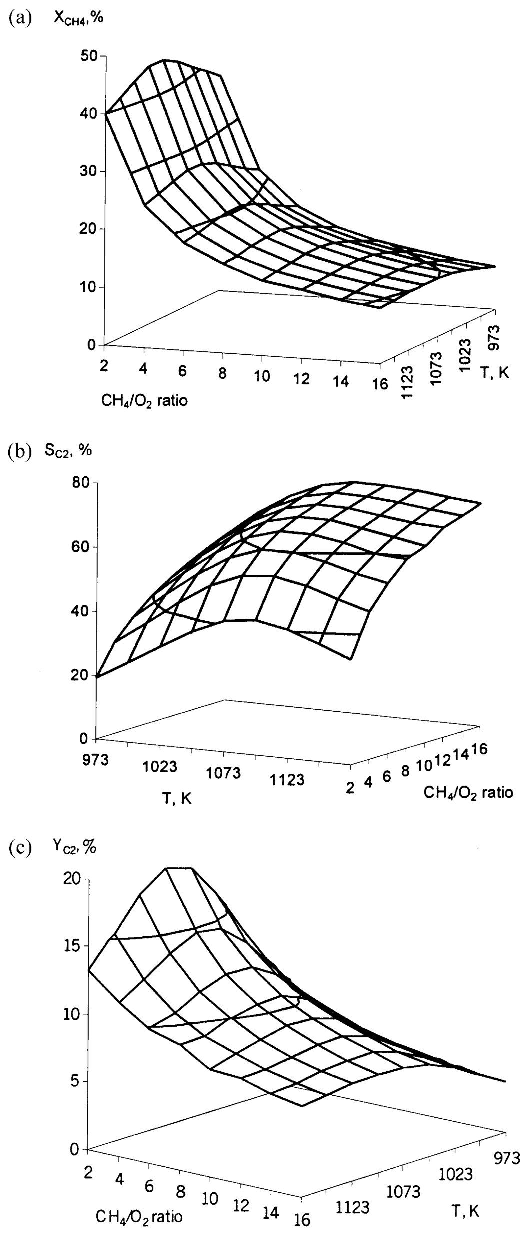

Fig. 1. Influence of CH_4/O_2 ratio and temperature on the (a) conversion of methane, (b) selectivity and (c) yield of C_2 product ($X_{O_2} = 100\%$, $c^0_{N_2} = 25\%$ and $P = 0.11$ MPa).

plotted starting from CH_4/O_2 feed ratio 2 in Fig. 1. This is because all the hydrocarbons in the process will be oxidized to carbon dioxides ultimately for the lesser CH_4/O_2 feed ratio (<2). Nevertheless, reduction in yield of C_2 product at higher selectivity, accomplished at high CH_4/O_2 feed ratio was due to insufficient oxygen in the reaction. As a result, a higher yield was obtained with higher oxygen concentration inspite of decrease in selectivity.

7.2. *Effect of temperature*

It is clear from Fig. 1, that a maxima was found for the conversion of methane, selectivity and yield of C_2 between temperature ranges of 973–1173 K. The optimum temperature was found around 1098 K. Conversion of methane at high CH_4/O_2 feed ratio within the temperature range did not change to significant extent. This was due to the low concentration of oxygen involved in the reactions. The selectivity as well as the yield of C_2 product at the reactor exit increased as the reaction temperature increased until 1098 K. At low temperature, there was a predominance of the heterogeneous kinetics over the gas-phase reaction and increasing the temperature enhanced the process. At high temperatures ($T > 1073$ K), the selectivity and yield benefit from the consecutive reactions caused by the gas-phase reaction and reached the maximum value. After the optimal temperature, the oxidation of C_2 started to predominate, which brings down the selectivity. As a result the yield of C_2 product decreased.

The maximum yield was obtained when the reactor was allowed to operate at the conditions such that total oxygen was consumed, i.e. 100% oxygen conversion. In order to obtain 100% conversion, different volummetric flow rate were used keeping the catalytic bed height constant. Conversion, C_2 yield and selectivity plots in Fig. 1 were obtained under these conditions. It shows that there was no optimum feed composition for a reactor that can be found from these graphs for OCM reaction using La_2O_3/CaO as catalyst since the yield keep dropping with the increase in concentration of methane in the feed.

7.3. *Effect of contact time*

Contact time has considerable influence on OCM process. Reactants would have longer contact time with low space velocity. The reaction would go to completion and the process will be enhanced. A comparison of reactor performance between temperature 1103 and 973 K under different contact times are shown in Fig. 2. It was found that oxygen already achieved total conversion at 20 kg s m^{-3} at 1103 K, and C_2 yield reached the maximum. At 973 K, conversion of oxygen increased gradually with the contact time. The course of methane conversion corresponded to that of oxygen. When oxygen conversion was complete, no further increase of methane conversion was found with contact time. Selectivity of ethylene increased with contact time while selectivity of ethane was found almost stable and dropped slightly with the contact time. The simulated results were in agreement with the experimental results reported by Stansch et al. [9].

7.4. *Effect of inert gas in the feed*

Most of the OCM processes were carried out in the presence of inert for dilution purpose. There was a noticeable increase in selectivity and yield to the point of total exhaustion of the oxygen supply reported under isothermal conditions when the diluents concentration was increased [2]. The presence of inert gas in the feed was also simulated under isothermal operation for its influence on conversion

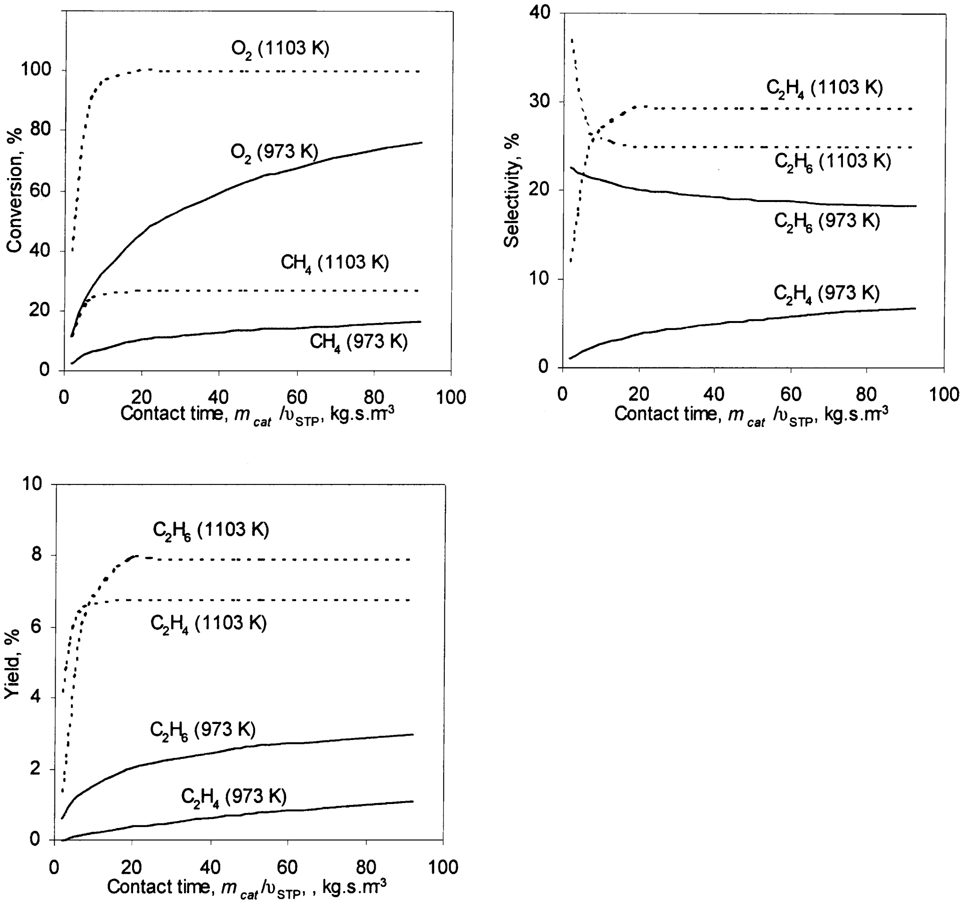

Fig. 2. Effect of contact time on the conversion of methane, selectivity and yield of C_2 product at 973 and 1103 K ($c^0_{CH_4} = 65\%$, $c^0_{O_2} = 15\%$ and $c^0_{N_2} = 20\%$).

and selectivity. The simulated inert was nitrogen gas. The results of the simulation are presented in Fig. 3.

Positive effects were noticed for the presence of inert gas N_2. It was observed that there is an optimal ratio for the inert gas in feed for OCM reaction. At 55% of N_2 gas in feed, the conversion of methane and oxygen as well as the yield of ethylene and ethane were found to be an optimum as shown in Fig. 3 under the condition of low CH_4/O_2 feed ratio 4. Increase of reactants conversion with the increase of diluents at first was due to the dilution effect of oxygen. This encouraged the methane coupling reaction while suppressed the deep oxidations. This resulted an increase in reactants conversion in addition to the yield of C_2 product while the selectivity remained almost constant. The reactants conversion and C_2 product yield dropped with an increase of nitrogen gas because further dilution restricted the deep oxidation as well as coupling oxidation reactions.

The OCM reaction can run using air and methane instead of methane, pure oxygen and nitrogen as an inert. In order to maintain the ratio 4, the closest achievable ratio of 55% of nitrogen in feed using methane and air was found to be methane to air ratio equals to 0.85, where nitrogen presents as 43% of feed. Due to the low concentration of oxygen involved in the OCM after dilution, this yield improvement was obtained at the expense of an increase in the reactor size for the same production rate.

7.5. *Effect of water (steam) in the feed*

Water is considered one of the products in the OCM reaction. Positive effects were noticed for the presence of water in the feed although it was small [11]. The conversion of methane as well as the yield of ethane and ethylene were found to increase with the increase of water presence in the feed. The influence of water in the conversion and yield is presented in Table 4. The increase of water concentration in feed had some dilution effect to the system. This resulted a slightly increase in the conversion of reactant and C_2 yield. Increasing the steam in feed after certain amount would encourage the steam reforming of ethylene (Step 8 of reaction scheme), resulting in the drop of ethylene yield. An optimum yield of ethylene was found with 20% water and 20% of nitrogen in the feed and CH_4/O_2 ratio of 4.

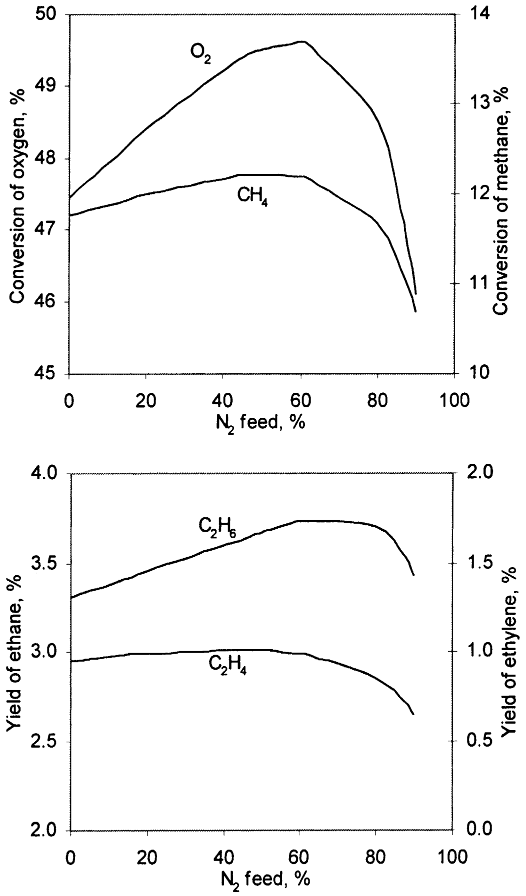

Fig. 3. Effect of N_2 gas present in feed on the conversion and yield of C_2 product ($CH_4/O_2 = 4$ and $T = 1023\,K$).

7.6. *Effect of carbon dioxide in the feed*

Carbon dioxide is one of the products in OCM reaction too. However, the presence of CO_2 has negative effect to the reaction. The presence of CO_2 in feed inhibits the overall rate in catalytic reaction; i.e. given the kinetic equations used in this work, all the component oxidation rates have negative power of CO_2. This causes a drop in conversion, selectivity and yield.

Table 4
Influence of water in the feed ($CH_4/O_2 = 4$, $T = 1023\,K$)

$c^0_{H_2O}$ (%)	X_{CH_4} (%)	X_{CH_4} (%)	$Y_{C_2H_6}$ (%)
$N_2 = 0\%$			
10	11.84	0.97	3.37
20	11.92	0.98	3.48
30	12.00	0.99	3.49
$N_2 = 20\%$			
10	12.06	1.00	3.52
20	12.12	1.01	3.58
30	12.14	1.00	3.64

7.7. *Adiabatic fixed bed reactor*

The OCM is an exothermic reaction. Temperature would rise in the reactor depending upon its operation. In adiabatic reactor, a rise in temperature can lead to a run away condition. The important consideration in the operation of an adiabatic reactor is to limit the hot spot and avoid excessive sensitivity to the variation in the parameters. It causes not only changes to the conversion, selectivity and yield of the reaction, but can lead to explosion if the temperature shoots extremely high.

7.8. *Effect of CH_4/O_2 ratio*

Fig. 4a shows the temperature profile in packed bed reactor under adiabatic operation. For low CH_4/O_2 ratio, the temperature shot up more than two-folds within a very short bed for OCM reaction. This resulted a hot spot formed at that point in the reactor. To limit the hot spot, shortening the catalyst bed or providing some arrangement of inter-cooling in the multistage catalytic bed reactor can control the reaction. It depends also on the feed temperature of reactants, the CH_4/O_2 feed ratio and dilution of the reactants.

For OCM reaction, increasing in temperature increased the reaction rates. The conversion of reactant, selectivity and yield of the product increased with an increase of temperature up to 1098 K. In adiabatic operation, heat released during oxidation coupling process increased the temperature as well as the rate of reactions. This doubled the reaction rates and heat release. For low CH_4/O_2 ratio (<6), temperature increased very sharp along the bed with its value $>1098\,K$, temperature which was found to be optimal under isothermal conditions. Temperature reached its maximum (2360 K for CH_4/O_2 of 2) at the point at 100% conversion of oxygen. Under the influence of high temperature, a large fraction of hydrocarbon was oxidized to CO_2. Most of ethane produced in the reaction would be dehydrogenated into ethylene because of high temperature. After the complete consumption of oxygen, C_2 hydrocarbon that formed during the reaction continue to undergo pyrolysis or steam-reforming of hydrocarbons which is endothermic until the exhaustion of ethylene and continued with a fast water shift gas reaction. The temperature dropped and reached a constant value after fully transformation from C_2 hydrocarbon into CO_x. This resulted in the drop of selectivity.

For high CH_4/O_2 ratio, (>8), temperature increased more gradually along the catalyst bed and was not critical. Selectivity of C_2 product reached >50% (Fig. 4b) and remained at high value. Fig. 4c shows generally longer bed did not favor the C_2 yield after the peak temperature. It would only further decrease the selectivity and C_2 yield for low CH_4/O_2 ratio. Therefore, high CH_4/O_2 ratio should be used under adiabatic operation to avoid hot spot and low C_2 yield. Nonetheless, C_2 yield obtained at high CH_4/O_2 ratio is still lower ($<10\%$) compared to the value obtained under isothermal condition. This was due to the low oxygen involved in the reaction.

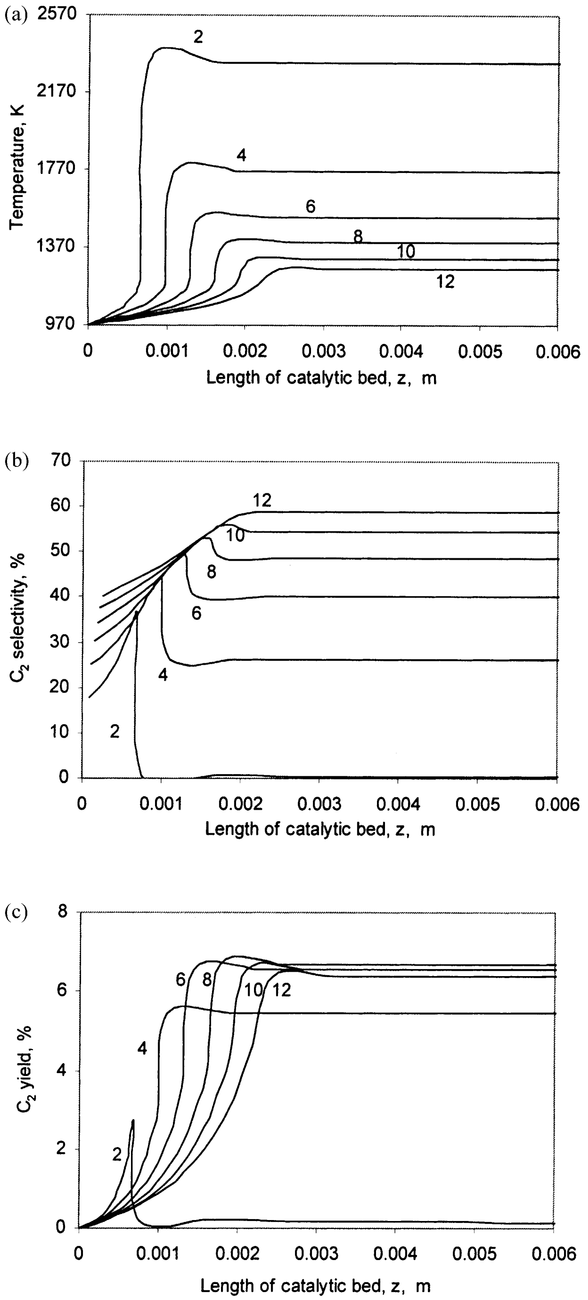

Fig. 4. (a) Temperature profile, (b) C_2 selectivity and (c) C_2 yield at different CH_4/O_2 feed ratios along the catalyst bed in adiabatic operation ($T^0 = 973\,K$, $c^0_{N_2} = 25\%$ and $m_{cat}/\upsilon_{STP} = 3.75\,kg\,s\,m^{-3}$).

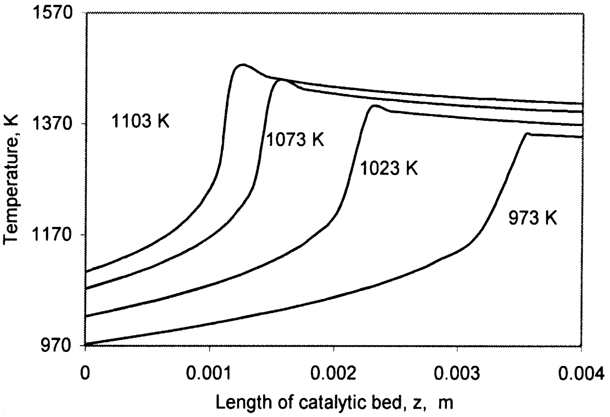

Fig. 5. Temperature profile along the catalyst bed in adiabatic operation at different feed temperatures ($CH_4/O_2 = 10$, $c^0_{N_2} = 25\%$ and $m_{cat}/\upsilon_{STP} = 3.75\,kg\,s\,m^{-3}$).

7.9. Effect of feed temperature

Lower feed temperatures could be used in adiabatic operation as compare to isothermal operation in order to obtain a similar yield under the same space velocity. The heat of reaction released in OCM increased the reaction temperature along the reactor. Fig. 5 shows the effect of feed temperature over reaction temperature. The maximum temperature was found to increase with the feed temperature. Bed length needed to achieve complete conversion of oxygen became shorter with the increase of feed temperature. Higher temperature (>1123 K) was not beneficial for the yield as well as extra longer bed. Longer bed could encourage the steam reforming reaction especially under high temperature. For the condition of low feed temperature (973 K), the temperature raise was suitable and utilization of catalyst bed provided better conversion and yield at the end compared to higher feed temperature operation. Under such condition, the bed length needed in order to achieve 100% conversion of oxygen is still much shorter compared to an identical condition in isothermal case due to the temperature rise in reactor. The best feed temperature would be 973 K. However, safety considerations as well as reactor materials compel strict limitations on the maximum temperature rise that can be controlled by an adequate choice of operating conditions [5].

7.10. Effect of contact time

Lower contact time was needed to achieve high oxygen conversion in adiabatic operation compared to isothermal operation. Oxygen reached 100% conversion at $3.75\,kg\,s\,m^{-3}$ with 973 K feed temperature. Under the same feed temperature and high CH_4/O_2 ratio of 10, contact time did not show significant difference in the yield and selectivity of the desired product after achieving 100% of oxygen consumption.

7.11. Dilution of reactants

Dilution of feed with inert is one of a method used for temperature control. This would have the same function as dilution of bed with uncatalytic particles like quartz in the bed. Higher nitrogen ratio in feed during the reaction distributes the temperature more evenly along the bed. This results in gentle temperature gradient. The reaction in the bed with longer contact time gives higher yield of C_2 product.

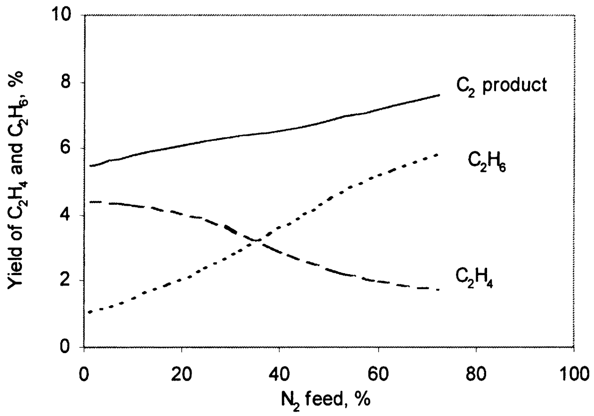

Fig. 6. Yield of C_2H_4 and C_2H_6 with different ratios of N_2 present in the feed ($CH_4/O_2 = 10$, $T^0 = 973\,K$ and $m_{cat}/\upsilon_{STP} = 3.75\,kg\,s\,m^{-3}$).

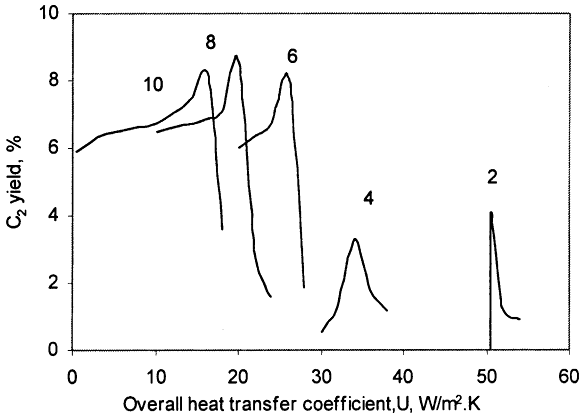

Fig. 7. Yield of C_2 profile with different overall heat transfer coefficient, U ($CH_4/O_2 = 10$, $T^0 = 973\,K$, $c^0_{N_2} = 25\%$ and $m_{cat}/\upsilon_{STP} = 1.75\,kg\,s\,m^{-3}$).

Nonetheless, higher C_2 yield was obtained under higher inert ratio with high ratio of ethane in the product (Fig. 6). This was due to the increment of temperature during the reaction. For lower inert ratio, higher reaction temperature would be achieved. This provides the locale which promotes the dehydrogenation of ethane and resulted in higher yield of ethylene as compare to ethane. When the inert ratio is high, reactants involved in reaction were less and subsequently less heat released. Thermal cracking was not significant and, therefore, most of the C_2 hydrocarbons stay as ethane. As a result, higher C_2 yield was obtained at high inert feed ratio with low C_2H_4/C_2H_6 ratio.

8. Non-adiabatic/non-isothermal operation

In an OCM process reactor, heat is generally removed during highly exothermic reaction. This can manipulate the reactor to operate under the desired conditions. Thus, the reactor can be operated under non-adiabatic/non-isothermal mode.

8.1. Role of overall heat transfer coefficient

Overall heat transfer coefficient, U, plays a crucial role in the non-isothermal reactor model. It represents the amount of heat to be removed from the system. Reactor working under appropriate overall heat transfer coefficient could produce optimum yield. Fig. 7 shows the peak of C_2 yield of different CH_4/O_2 ratio at particular value of U. Generally at the lower U value before each peak, the peak temperature achieved in the reactor was higher than the optimum temperature (1098 K). Increasing the value of U, decreased the peak temperature while increased the desired product yield. When the peak temperature dropped around 1098 K, the C_2 yield would reach a maximum value. The peak temperature produced at higher U value was lower than the optimum temperature (1098 K) and even lower than the ignition temperature for OCM reaction. It caused a steep drop in yield of C_2 hydrocarbons. Therefore, proper reactor operating conditions manipulation and value of U are paramount important in non-isothermal operation. Fig. 7 shows that higher optimum C_2 yield was obtained at high CH_4/O_2 ratio.

8.2. Effect of tube diameter

The use of fixed bed reactor lead to multitubular reactors with small tube diameter and a large number of tubes. Effect of tube diameter was studied under non-isothermal/non-adiabatic mode which is closer to practical operating conditions. The tube diameter has to be kept small in order to avoid steep axial and radial temperature gradients and to avoid reactor run-away condition [1]. Bigger tube diameter leads to higher temperature. This was due to more reactions occurring at a same surface area in catalyst bed and more heat was released at the same time. Temperature is the main controlling factor for C_2 yield in OCM process. If the system peak temperature has

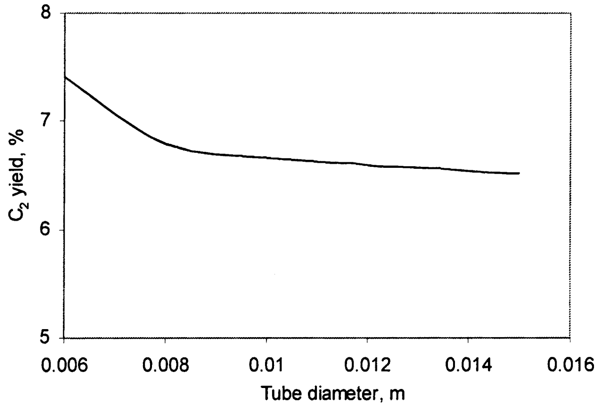

Fig. 8. Yield of C_2 product with different reactor tube diameter ($CH_4/O_2 = 10$, $T^0 = 973\,K$, $U = 14\,W/m^2\,K$, $c^0_{N_2} = 25\%$ and $m_{cat}/\upsilon_{STP} = 1.75\,kg\,s\,m^{-3}$).

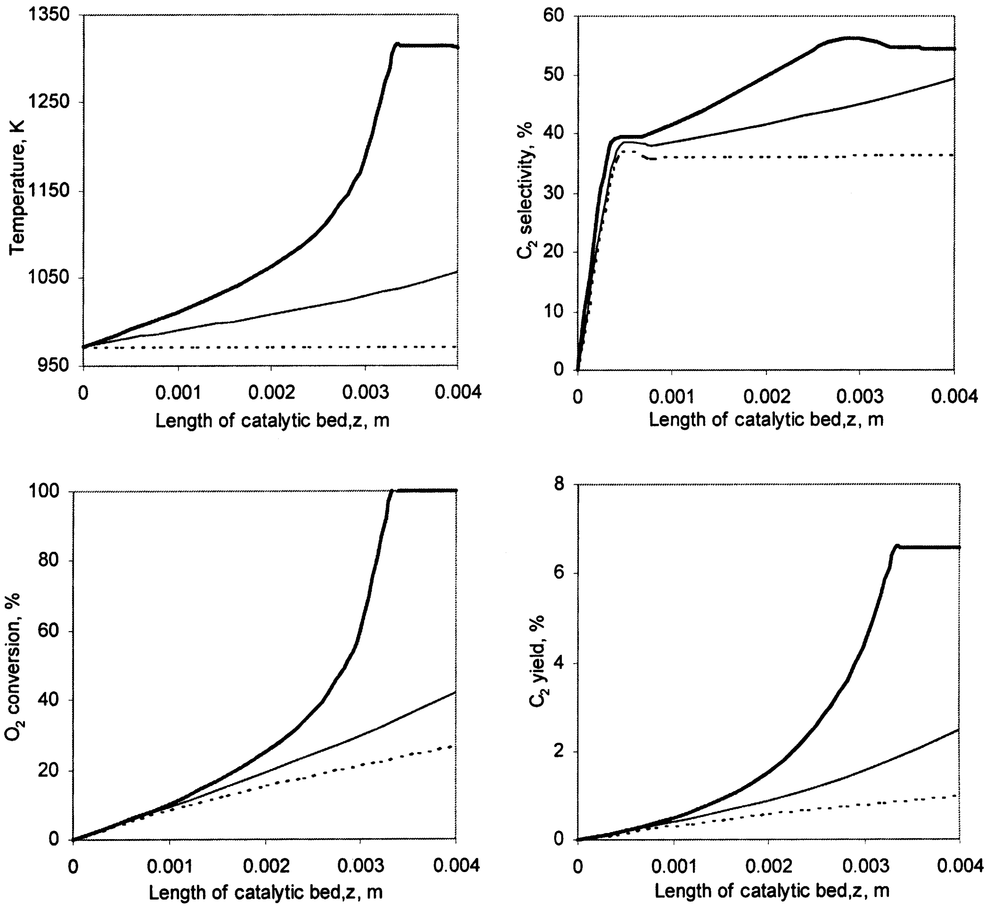

Fig. 9. Comparison between non-isothermal, adiabatic and isothermal operation ($T^0 = 973\,K$, ($CH_4/O_2 = 10$, $c^0_{N_2} = 25\%$, $m_{cat}/\upsilon_{STP} = 3.75\,kg\,s\,m^{-3}$, $U = 14\,W\,m^{-2}\,K$, for non-isothermal and non-adiabatic, (isothermal; adiabatic; non-isothermal/non-adiabatic)).

not reached the optimum temperature, increasing the tube diameter would produce better yield otherwise it would generate negative effect to the yield and depends on the operating conditions. Dautzenberg et al. [12] reported a multitubular reactor design with 2000 tubes of diameter 24 mm and length 2 m for OCM reactor on industrial scale. Fig. 8 shows the effect of tube diameter on C_2 yield. It shows that increasing the reactor diameter causing a drop in the C_2 yield and reached a constant value. The balance of mass and heat radial dispersion maintained the C_2 yield.

9. Comparison of the operation modes

It is interesting to compare isothermal, adiabatic and non-isothermal/non-adiabatic operations under steady state in terms of the conversion, selectivity and yield obtained in OCM. Fig. 9 presents the results of the comparison under the same feed conditions. The OCM process was simulated under conditions of high CH_4/O_2 ratio of 10 with 25% of inert and feed temperature of 973 K. This was due to adiabatic mode, which is not suitable to run under low methane to oxygen ratio. These operation modes were simulated for a short catalyst bed height of 0.004 m. The catalyst bed height was taken small to avoid the run away conditions. The longer bed height promotes steam reforming of ethylene under high temperature under adiabatic conditions.

It can be seen from the figure that the increased temperature in both non-isothermal and adiabatic cases gave rise to a considerably higher conversion and selectivity profile, as compared to the isothermal operation. Since high CH_4/O_2 ratio (=10) and short bed was simulated, the maximum yield achieved in isothermal condition was low. It was only 1% yield of C_2 product. Higher yield was attained in non-isothermal conditions. It was 6.5 and 2.5% in adiabatic and non-isothermal/non-adiabatic modes, respectively.

10. Conclusion

The present study has shown that temperature was a sensitive parameter in OCM reaction. Adiabatic and non-isothermal mode produced low C_2 yield for OCM although they were controlled from run away situation. The OCM process operating under low CH_4/O_2 ratio at an optimum temperature using La_2O_3/CaO catalyst in a fixed bed reactor still did not produce C_2 yield >25%. Other catalysts and reactor configuration should be investigated in order to produce higher C_2 yield.

Acknowledgements

The Financial support from Ministry of Science, Technology and Environment, Malaysia under long term IRPA grant (Project no. 02-02-05-7003) is acknowledged.

References

[1] L. Mleczko, M. Baerns, Fuel Proc. Tech. 42 (1995) 217–248.
[2] Y.K. Kao, L. Lei, Y.S. Lin, Ind. Eng. Chem. Res. 36 (1997) 3583–3593.
[3] V.R. Choudhary, B.S. Uphade, S.A.R. Mulia, Ind. Eng. Chem. Res. 36 (1997) 3594–3601.
[4] P.J. Gellings, J.M.B. Henny, Catal. Today. 58 (2000) 1–53.
[5] J.M. Santamaria, E.E. Miro, E.E. Wolf, Ind. Eng. Chem. Res. 30 (1991) 1157–1165.
[6] J.H.B.J. Hoebink, P.M. Couwenberg, G.B. Marin, Chem. Eng. Sci. 49 (24B) (1994) 5453–5463.
[7] Y. Mortazavt, R.R. Hudgins, P.L. Silveston, Can. Chem. Eng. J. 74 (1996) 683–694.
[8] J. Coronas, A. Gonzalo, D. Lafarga, M. Meněndaz, AIChE J. 43 (11) (1997) 3095–3104.
[9] Z. Stansch, L. Mleczko, M. Baerns, Ind. Eng. Chem. Res. 36 (1997) 2568–2579.
[10] Z. Stansch, Kinetics for oxidative coupling of methane process over La_2O_3/Ca-O catalyst, Ph.D. thesis, Ruhr-University Bochum, Bochum, 1995.
[11] B. Zhou, A.M. Richard, K.J. Smith, Can. Chem. Eng. J. 73 (1995) 103–109.
[12] F.M. Dautzenberg, J.C. Schlatter, J.M. Fox, J.R. Rostrup-Nielsen, L.J. Christiansen, Catal. Today 13 (1992) 503–509.